**Article ID**: 1000-9116(2003)01-0016-10

# Mapping crustal S-wave velocity structure with SV-component receiver function method*

ZOU Zui-hong (邹最红) CHEN Xiao-fei (陈晓非)
*Department of Geophysics, Peking University, Beijing* 100871, *China*

**Abstract**

In this article, we analyze the characters of SV-component receiver function of teleseismic body waves and its advantages in mapping the S-wave velocity structure of crust in detail. Similar to radial receiver function, SV-component receiver function can be obtained by directly deconvolving the P-component from the SV-component of teleseismic recordings. Our analyses indicate that the change of amplitude of SV-component receiver function against the change of epicentral distance is less than that of radial receiver function. Moreover, the waveform of SV-component receiver function is simpler than the radial receiver function and gives prominence to the PS converted phases that are the most sensitive to the shear wave velocity structure in the inversion. The synthetic tests show that the convergence of SV-component receiver function inversion is faster than that of the radial receiver function inversion. As an example, we investigate the S-wave velocity structure beneath HIA station by using the SV-component receiver function inversion method.

**Key words: receiver function; SV-component receiver function; S-wave velocity structure inversion**
**CLC number**: P315.3$^{+}$1 **Document code**: A

## Introduction

Since the conception of receiver function was introduced by Langston, the inversion technique of radial receiver function of teleseismic body waves has been widely used, and many fruits in mapping the structure of crust and upper mantle have been achieved (Langston, 1979; Owens, *et al*, 1984, 1987; Ammon, 1991; Ammon, *et al*, 1990; Kind, *et al*, 1995). Many Chinese researchers have also done many studies in this field. WU and ZENG (1998) applied the techniques of time domain Wiener deconvolution and the maximum entropy deconvolution to isolate receiver function from teleseismic waveforms. Zhao and Frohlich (1996) made improvement on receiver function methods by convolving vertical component with transfer function to obtain radial component to delineate crustal structure. LIU, *et al* (1996, 1997, 2000) incorporated the maximal likelihood estimation of the complex receiver function spectrum ratio with the nonlinear inversion technique to improve the inversion results. Similar to the radial receiver function method (Langston, 1979), Kosarev, *et al* proposed *Q*-component receiver function to study earth structure, which is derived by filtering the waveforms of P and SV components of teleseismic body waves with Berkhout's deconvolution filtering technique (Berkhout, 1977; Kosarev, *et al*, 1993; Petersen, *et al*, 1993; Kind, *et al*, 1995; Farra, Vinnik, 2000). In this article, we shall apply directly the ma-

* **Received date**: 2002-05-23; **revised date**: 2002-08-12; **accepted date**: 2002-08-12.
**Foundation item**: State Key Basic Research Development and Programming Project (G199804070201) and State Natural Science Foundation (40074008).

ture isolation technique of radial receiver function to the isolation of SV-component receiver function and investigate its characters and merits in the inversion.

# 1 The fundamentals of radial receiver function and its isolation technique

The vertical and radial components of the response at a station due to a teleseismic P wave can be theoretically represented by

$$\begin{cases} D_{\mathrm{V}}(t) = I(t) * S(t) * E_{\mathrm{V}}(t) \\ D_{\mathrm{R}}(t) = I(t) * S(t) * E_{\mathrm{R}}(t) \end{cases} \tag{1}$$

where, $D_{\mathrm{V}}(t)$ and $D_{\mathrm{R}}(t)$ denote, respectively, the vertical and radial displacement; $S(t)$ is the effective seismic source function; $I(t)$ is the impulse response of the recording instrument; $E_{\mathrm{V}}(t)$ and $E_{\mathrm{R}}(t)$ are the vertical and radial impulse response of crust structure. In frequency domain, the process above is given by

$$\begin{cases} D_{\mathrm{V}}(w) = I(w)S(w)E_{\mathrm{V}}(w) \\ D_{\mathrm{R}}(w) = I(w)S(w)E_{\mathrm{R}}(w) \end{cases} \tag{2}$$

According to Langston (1979), radial receiver function is defined in frequency domain as follows:

$$E'_{\mathrm{R}}(w) = \frac{E_{\mathrm{R}}(w)}{E_{\mathrm{V}}(w)} = \frac{D_{\mathrm{R}}(w)}{D_{\mathrm{V}}(w)} \tag{3}$$

As to the teleseismic wave with large enough epicentral distance, P wave is almost vertically incident beneath the station. So it implies

$$E_{\mathrm{V}}(t) \approx d(t)$$

that is $E_{\mathrm{V}}(w) \approx 1$. Therefore we have

$$E'_{\mathrm{R}}(w) \approx E_{\mathrm{R}}(w) \tag{4}$$

Transforming $E'_{\mathrm{R}}(w)$ to time domain yields $E'_{\mathrm{R}}(t)$, that is the radial receiver function. Obviously, it only includes the information about the earth structure beneath the station and does not include the information about the seismic source. Due to this property of the radial receiver function, crustal structure beneath the station can be imaged by fitting the observed receiver function and the synthetic receiver function calculated according to certain crust structure models (Langston, 1979; Owens, *et al*, 1984; Ammon, *et al*, 1990). This technique has caught much attention due to its simplicity, easy realization and effectiveness. Now it has become one of the important techniques to study the crust structure.

Usually in order to remove the influence of random noises, when we delineate the earth structure with the inversion of the radial receiver functions, we need to use mean radial receiver function which is obtained by stacking the several events radial receiver functions from different epicentral distances (Owens, *et al*, 1984; Ammon, 1991). If the radial receiver functions have nothing with the epicentral distances, this stacking is doubtlessly right. But as a matter of fact, radial receiver function is the function of epicentral distances and when the epicentral distances become small, the radial receiver functions become more sensitive to the epicentral distances. As to the single layer crust model in Figure 1, we give the change of the radial receiver function

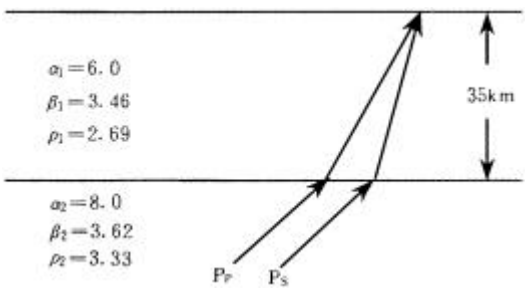


Figure 1 Single-layer crustal structure model

waveform against the P-wave's incident angle at the bottom of the crust (see Figure 2). The approach taken here to isolate the receiver functions is the one suggested by Ammon (1991) that preserves the absolute amplitude of receiver functions. From Figure 2 we can see that the radial receiver function is changing against the incident angle. Accordingly, if the epicentral distance is not bounded within certain small range, the resultant deviation of the mean of stacking receiver functions will be greater than the random noises, consequently, the mean of stacking receiver functions could not represent the true receiver function related to the earth structure. On the other hand, if the epicentral distances are bounded within a small range, the data that can be used in the stacking will be reduced greatly and cannot effectively remove the random noises. It is the limitation of the radial receiver function technique.

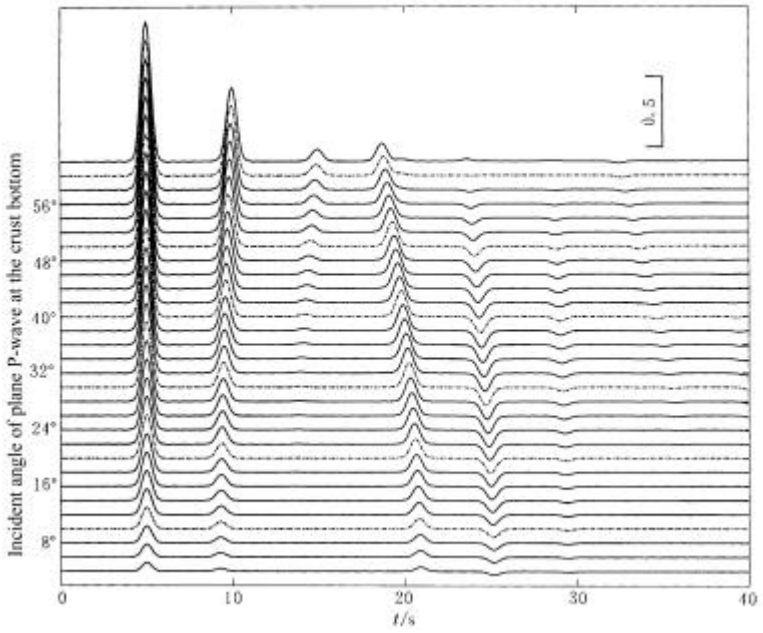


Figure 2 The waveform of radial receiver function waveform against the P-wave's incident angle at the bottom of the single-layer crust model shown in Figure 1
Radial receiver functions change in accord with the change of incident angle from 4° to 62° with an interval of 2°. The six dotted lines represent the radial receiver functions corresponding to the incident angle of 10°, 20°, 30°, 40°, 50° and 60°

## 2 The isolation method and synthetic test of SV-component receiver function

In order to relax the radial receiver function's limitation mentioned above, with a similar manner as to Kosarev, *et al* (1993) did, we transform the V-R-T coordinate to the P-SV-SH coor-

dinate according to the seismic recording below

$$\begin{cases} D_{\mathrm{P}}(t) = D_{\mathrm{V}}(t)\cos j + D_{\mathrm{R}}(t)\sin j \\ D_{\mathrm{SV}}(t) = -D_{\mathrm{V}}(t)\sin j + D_{\mathrm{R}}(t)\cos j \end{cases} \tag{5}$$

where, $j$ is the take off angle of station recording and it can be determined according to the maximum vertical and radial amplitude of the direct P-wave within the first period (Figure 3), that is

$$j = \arctan\left(\frac{R_0}{V_0}\right) \tag{6}$$

In the P-SV-SH coordinate, we have

$$\begin{cases} D_{\mathrm{P}}(t) = S(t) * I(t) * E_{\mathrm{P}}(t) \\ D_{\mathrm{SV}}(t) = S(t) * I(t) * E_{\mathrm{SV}}(t) \end{cases} \tag{7}$$

where $E_{\mathrm{P}}(t)$ and $E_{\mathrm{SV}}(t)$ represent the P-component and SV-component of impulse response of the crust structure, respectively. Similar to the radial receiver function (Langston, 1979), SV-component receiver function can be defined in frequency domain by

$$E'_{\mathrm{SV}}(w) = \frac{E_{\mathrm{SV}}(w)}{E_{\mathrm{P}}(w)} = \frac{D_{\mathrm{SV}}(w)}{D_{\mathrm{P}}(w)} \tag{8}$$

Transforming it into time domain yields $E'_{\mathrm{SV}}(t)$ which is the SV-component receiver function. In the P-SV-SH coordinate, the direct P-wave is always recorded at the $P$-axis totally, so $E_{\mathrm{P}}(t) \approx d(t)$, which means $E'_{\mathrm{SV}}(w) \approx E_{\mathrm{SV}}(w)$ is always hold whether the take off angle is nearly vertical or not. Moreover, since SV-component receiver function is obtained by deconvolving the P-component from the SV-component, it removes the problem of varying projections of seismic phases on the vertical and radial component for different take off angles, which cause the amplitudes of receiver functions change greatly in the radial receiver function. Therefore, the amplitude change of SV-component receiver function against the incident angle is smaller than that of the radial receiver function.

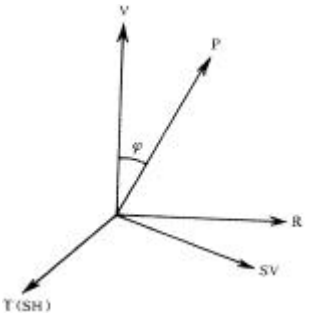


Figure 3 Transformation from coordinate V-R-T to coordinate P-SV-SH

In Figure 4 we compare the radial receiver function with the SV-component receiver function according to the same single layer crust model. It shows that the amplitude change of SV-component receiver function against the incident angle (epicentral distance) is obviously smaller than that of radial receiver function. Therefore, for the case of multi-events with certain epicentral span, the stacked SV-component receiver function exhibits more accurately the crustal structure information than the stacked radial receiver function. Additionally, waveform feature of SV-component receiver function is simpler than that of the radial receiver function. In SV-component receiver function, the direct P-wave disappears and the multiple P-waves nearly disappear, because the direct P-wave projects nothing on SV-polarization. According to Owens, *et al* (1984), receiver function is most sensitive to the P-SV conversion phase and the velocity structure of shear wave is not sensitive to the waveform of direct P-wave which although has large amplitude. Therefore, the simple wave-

form of the SV-component receiver function does not lack the useful information of shear wave velocity structure, whereas it speeds up the inversion process for without fitting the waveform of direct P-wave.

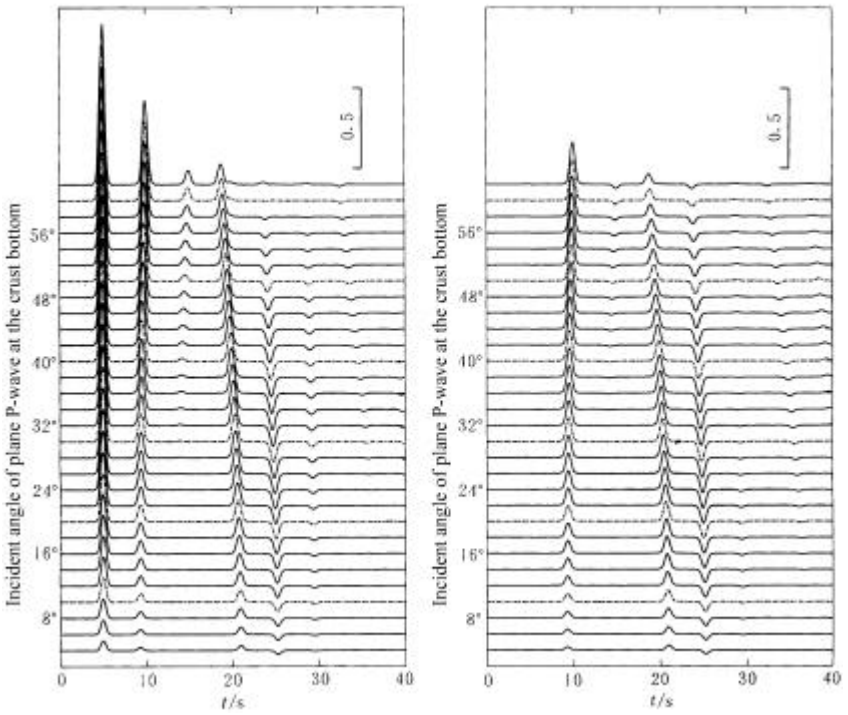


Figure 4 Comparison between the radial receiver function and the SV-component receiver function against the P-wave's incident angle at the bottom of the single-layer crustal model showed in Figure 1

The left part is radial receiver function and the right part is SV-component receiver function. The range of incident angle is from 4° to 62° with interval of 2°, and the six dotted lines represent the receiver functions corresponding to the incident angle of 10°, 20°, 30°, 40°, 50° and 60°

Regarding the synthetic receiver function as "observed" receiver function, we obtain the inversion result showed in Figure 5 by using a nonlinear inversion algorithm that combines the BFGS iterative scheme (a quasi-Newton algorithm) and the trust region strategy (YUAN, SUN, 1997). The synthetic receiver function used in Figure 5 is calculated for the case in which the incident angle beneath the crustal bottom is 20°. Figure 5c and 5d show the change of the objective function against the number of iteration in the inversion process. From Figure 5 we can see that both inversion results fit the true model very well, whereas, the inversion result of the SV-component receiver function is a little worse than the radial receiver function at the bottom since SV-component receiver function lacks the information about the direct P-wave. Fortunately, the difference is too small to be meaningful, which indicates the information of the direct P-wave is not very sensitive to the S-wave velocity structure. We can see, however, that the convergence speed of the nonlinear inversion process with SV-component receiver function is faster than that with radial receiver function. The iteration number with SV-component receiver function is about three fourths of that with radial receiver function.

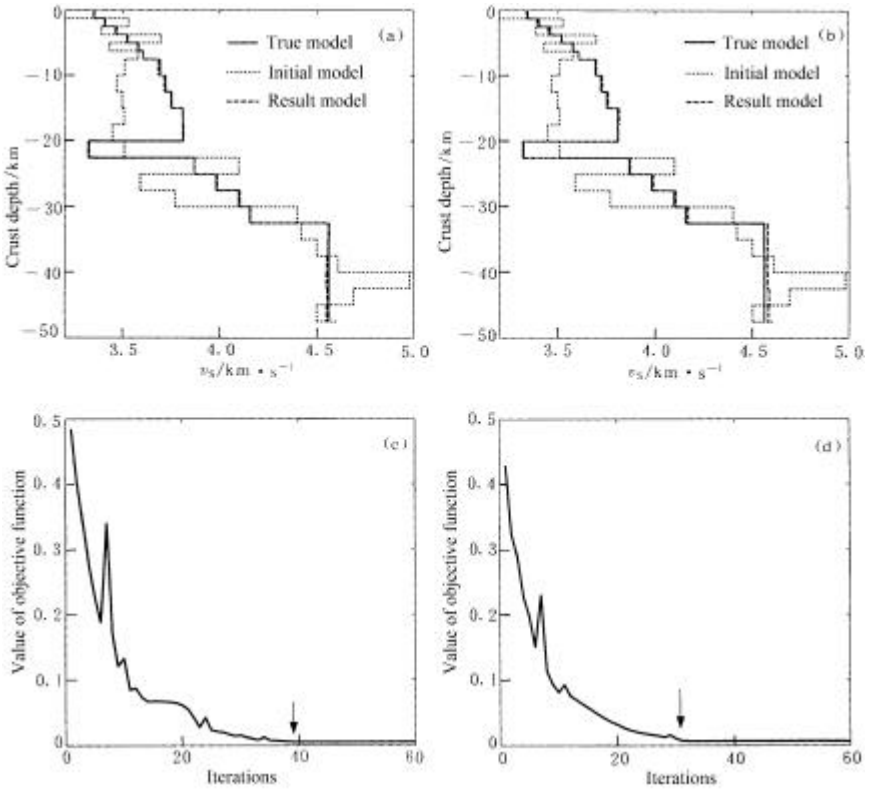


Figure 5 Inversion results and the corresponding inversion iteration process of the synthetic test where the incident angle of direct-P wave at the bottom of the crustal model showed in this figure is 20°

(a) and (b) are the inversion results of the radial receiver function and SV-component receiver function, respectively; (c) and (d) show the change of objective function against inversion iteration process

In order to indicate the influence of the stability of SV-component receiver function's amplitude with respect to the change of epicentral distance on the structure inversion results we run the inversion with stacked synthetic SV-component receiver functions with different incident angles at the bottom of crust. We consider three cases: a) the incident angles of the receiver functions stacked are 20° and 25°, respectively; b) the incident angles of the receiver functions stacked are 20°, 25° and 30°, respectively; and c) the incident angles of the receiver functions stacked are 20°, 25°, 30° and 35°, respectively. The inversion results are showed in Figure 6. For the first two cases, both inversion results fit the true model very well, but they are slightly worse than that for the case of single incident angle showed in Figure 5. As to the third case, although both inversion results of radial and SV-component receiver functions cannot fit the true model very well, we can see the inversion result of SV-component receiver function is better than that of the radial receiver function. Therefore, to obtain a satisfactory inversion result, we should select the events whose epicentral distances range is as small as possible. Nevertheless, as for the same discrepant range of epicentral distances, the inversion result of SV-component receiver function is better than that of radial receiver function. In Table 1, we list the iterations and the final objective functions corresponding to each inversion result in Figure 6. It can be seen that the convergence of SV-component receiver function is faster and better than the radial receiver function in all the three cases.

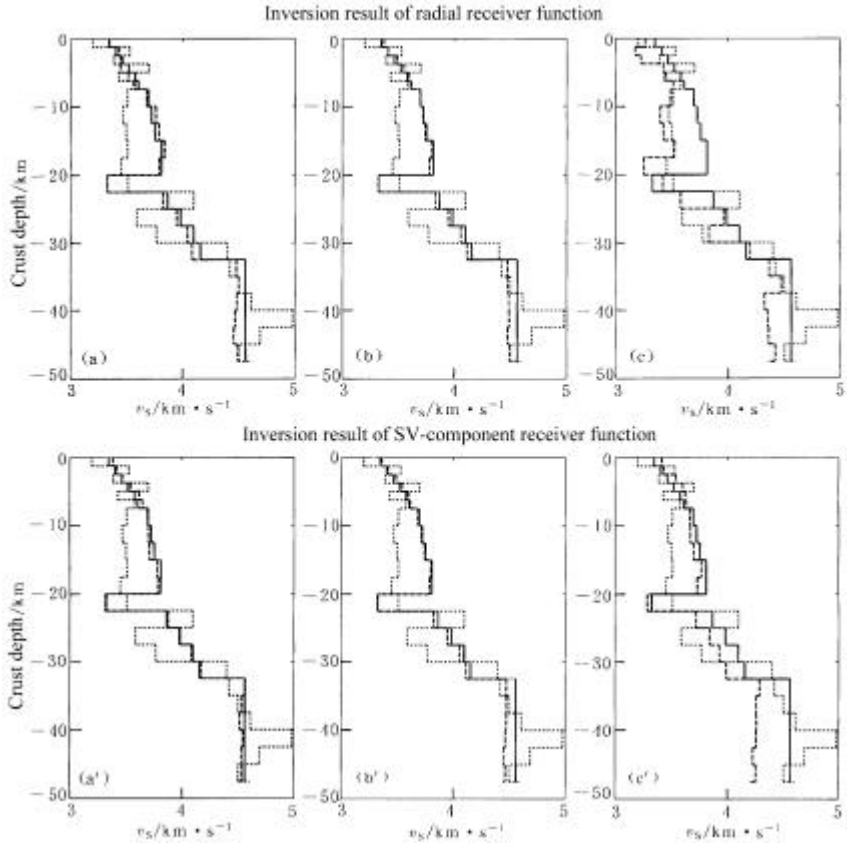


Figure 6 Inversion results of the first (a, a′), the second (b, b′) and the third case (c, c′)

Table 1 Iterations and final objective function corresponding to inversion result in Figure 6

| | Number of iterations | | Objective function | |
|---|---|---|---|---|
| | Radial receiver function | SV receiver function | Radial receiver function | SV receiver function |
| Case 1 | 50 | 30 | 0.03 | 0.02 |
| Case 2 | 30 | 20 | 0.03 | 0.02 |
| Case 3 | 80 | 20 | 0.13 | 0.06 |

## 3 An inversion example with SV-component receiver function

Now with an example we show the isolation of the SV-component receiver function from the observed seismograms, the corresponding inversion results and the comparisons with those obtained from the radial receiver functions. Usually, observed seismograms are recorded at geographic coordinate (V, N and E). In the radial receiver function technique, the geographic coordinate (V, N and E) are transformed into the V-R-T coordinate according to the back azimuth. In SV-component receiver function technique, however, the three components in V-R-T coordinate are further transformed into the P-SV-SH coordinate to isolate SV-component receiver function according to equation (8), where *P*-axis is determined by the maximum amplitude of the direct P-wave in the first period. As an example, in Figure 7, we give the radial and SV-component receiver functions from 5 events recorded at HIA station from the roughly same azimuth. These events are listed in Table 2. Figure 7a is the radial receiver functions and Figure 7c is the SV-

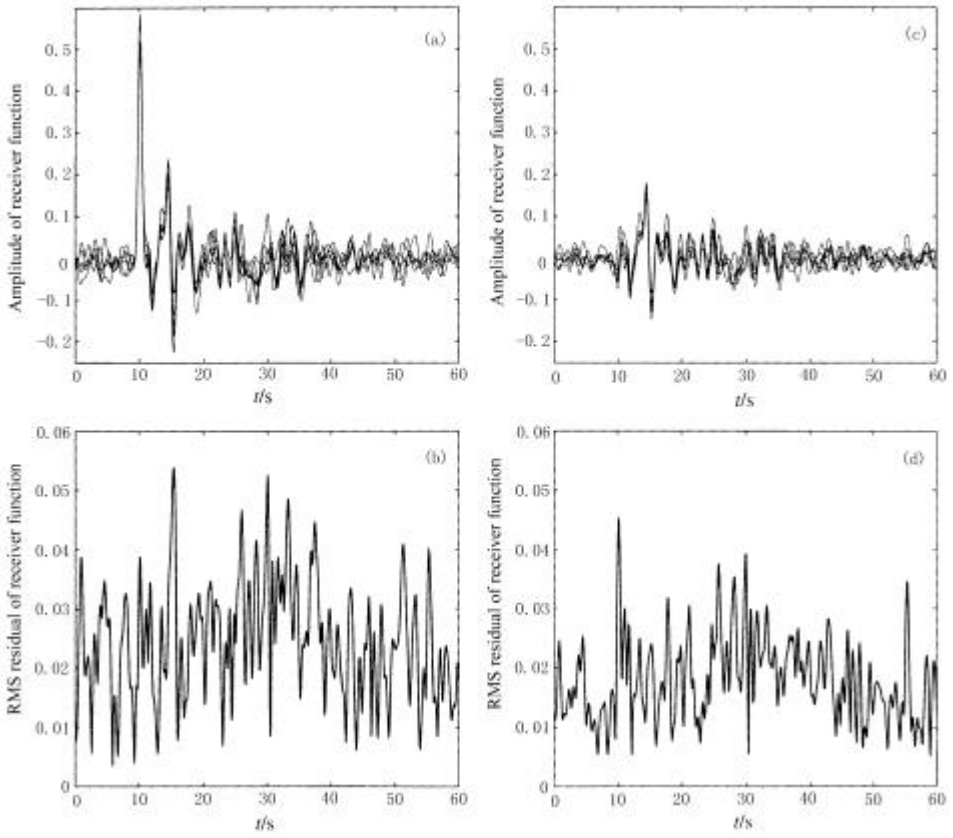


Figure 7 Receiver function isolated form five events recorded at HIA station
(a) and (b) are the radial receiver functions and the corresponding root-mean-square residual; (c) and (d) are the SV-component receiver functions and the corresponding root-mean-square residual

component receiver functions, where the dotted line is the mean receiver function. From Figure 7a and 7b we can see the amplitude change of the radial receiver functions is greater than that of the SV-component receiver function, and such character can also be seen from Figure 7b and 7d which are the root-mean-square residual of the receiver functions. Furthermore, the waveform of SV-component receiver function displays a simpler feature than the radial receiver function, which gives prominence to the PS converted phases that are the most sensitive to the shear wave velocity structure. The inversion results of the radial and SV-component receiver functions are given in Figure 8, where the initial model is determined on the base of the S-wave velocity structures beneath HIA station obtained by LIU, *et al* (1997) and by Mangino (1999) with radial receiver function method. According to the result of some former researchers, there exits high velocity layer at the depth of 3~4 km beneath the HIA station. Our result shows that the high velocity layer at the depth of 3~4 km beneath the HIA station is not very distinct and there exits low velocity in the middle crust and the Moho-discontinuity is about at the depth of 35 km or so. Comparisons between the inversion result of radial receiver function and that of SV-component receiver function show both methods turn out similar inversion results, but the result of SV-component receiver function is better. The comparison in convergence property shows that the inversion iterating converge after the 50th iteration in the SV-component receiver function inversion, whereas it needs

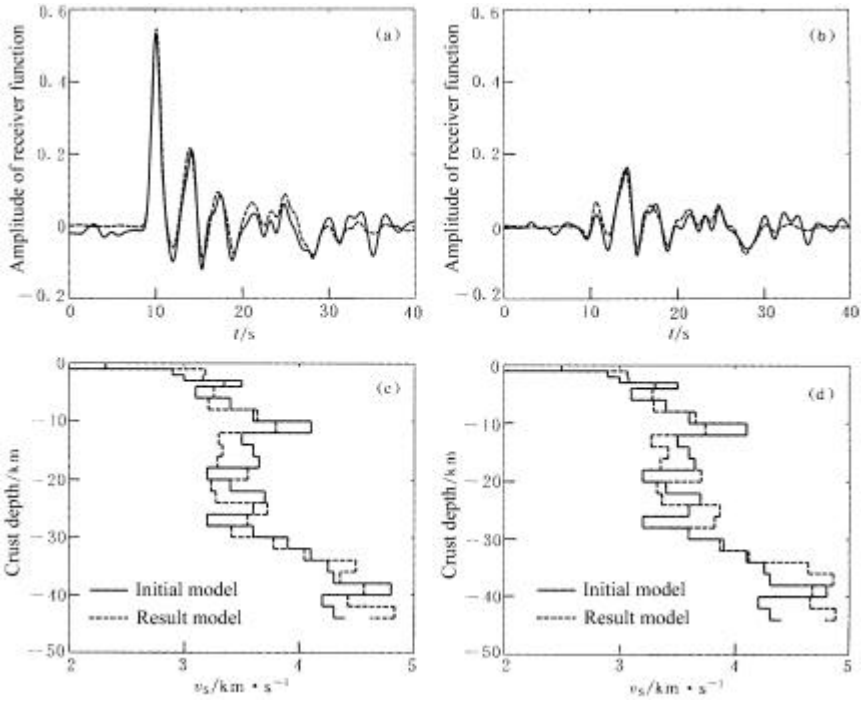


Figure 8 Inversion results of HIA station

(a) and (b) show the waveform fittings of final resultant models obtained by, respectively, the radial receiver function method and the SV-component receiver function method. The solid lines are the observed receiver function and the dashed lines are the synthetic receiver functions calculated by the final resultant models; (c) and (d) show the final resultant shear wave velocity models

Table 2 Seismic events used in isolating receiver functions

| No. | Date a-mo-d | Origin time h:min:s | $l_E$/(°) | $j_N$/(°) | Epicentral distance /km | $M$ |
|---|---|---|---|---|---|---|
| 1 | 1988-12-07 | 07:41:24 | 44.185 | 40.987 | 5 761 | 6.2 |
| 2 | 1989-09-17 | 00:53:39 | 51.749 | 40.203 | 5 291 | 6.1 |
| 3 | 1991-04-29 | 09:12:47 | 43.673 | 42.453 | 5 701 | 6.2 |
| 4 | 1991-06-15 | 00:59:20 | 44.009 | 42.461 | 5 682 | 6.1 |
| 5 | 1992-03-13 | 17:18:39 | 39.605 | 39.710 | 6 161 | 6.2 |

almost 100 iterations to make the inversion iterating converge in the radial receiver function inversion, which is consistent with our synthetic tests showed earlier.

# 4 Conclusion

In this article, we isolated the SV-component receiver function by deconvolving the P component from the SV component of teleseismic body-wave's recordings, and analyzed its property and advantage in mapping the shear wave velocity structure. We found: a) The amplitude change of SV-component receiver function against epicentral distance is less than that of radial receiver function, accordingly the root-mean-square residual of SV-component receiver function is smaller than that of radial receiver function; b) The waveform of SV-component receiver function is simpler than that of radial receiver function, and gives prominence to the PS converted phases which are the most sensitive to the shear wave velocity structure. The synthetic tests show that when the

stacked receiver function is derived from the events with larger epicentral distance range, the inversion results of SV-component receiver function is better than that of the radial receiver function; when the epicentral distance range is smaller, both inversion results are comparable. However, the convergence property of SV-component is better than that of radial receiver function. As an example, we investigate the shear wave velocity structure beneath HIA station by using this new inversion method with CDSN waveform data. The inversion result indicates the existence of a high velocity layer at the depth of 3~4 km and a low velocity zone in the middle crust; and shows the Moho-discontinuity is about at the depth of 35 km or so.

**Acknowledgements** The authors would like to express their gratitude to Prof. LIU Qi-yuan for his constructive comments.

## References

Ammon C J. 1991. The isolation of receiver effects from teleseismic P waveforms [J]. *Bull Seism Soc Amer*, **81**: 2 504~2 510.

Ammon C J, George E R, George Z. 1990. On the non-uniqueness of receiver function inversions [J]. *J Geophys Res*, **95**: 15 303~15 318.

Berkhout A. 1977. Least square inverse filtering and wavelet deconvolution [J]. *Geophys*, **42**: 1 369~1 383.

Farra V, Vinnik L P. 2000. Upper mantle stratification by P and S receiver functions [J]. *Geophys J Int*, **141**: 699~712.

Kind R, Kosarev G L, Petersen N V. 1995. Receiver functions at the stations of the German Regional Seismic Network (GRSN) [J]. *Geophys J Int*, **121**: 191~202.

Kosarev G L, Petersen N V, Vinnik L P. 1993. Receiver functions for the Tien Shan analog broadband network: Contrasts in the evolution of structures across the Talasso-Fergana fault [J]. *J Geophys Res*, **98**: 4 437~4 448.

Langston C A. 1979. Structure under Mount Rainier, Washington, inferred from teleseismic body waves [J]. *J Geophys Res*, **84**: 4 749~4 762.

LIU Qi-yuan, Kind R, LI Shun-cheng. 1996. Maximal likelihood estimation and nonlinear inversion of the complex receiver function spectrum ratio [J]. *Acta Geophysics Sinica*, **39**(4): 500~511 (in Chinese).

LIU Qi-yuan, Kind R, LI Shun-cheng. 1997. The receiver functions at the stations of the Chinese digital seismic network (CDSN) and their nonlinear inversion [J]. *Acta Geophysics Sinica*, **40**(3): 356~368 (in Chinese).

LIU Qi-yuan, CHEN Jiu-hui, LI Shun-cheng, *et al*. 2000. Passive seismic experiment in Xinjiang Jiashi strong earthquake region and discussion on its seismic genesis [J]. *Acta Geophysics Sinica*, **43**(3): 356~365 (in Chinese).

Mangino S. 1999. The receiver structure beneath the China Digital Seismograph Network stations [J]. *Bull Seism Soc Amer*, **89**: 1 053~1 076.

Owens T J, Steven R T, George Z. 1987. Crustal structure at regional seismic test network stations determined from inversion of broadband teleseismic P waves [J]. *Bull Seism Soc Amer*, **77**: 631~662.

Owens T J, Zandt G, Steven R T. 1984. Seismic evidence for an ancient rife beneath the Cumberland plateau, Tennessee: A detailed analysis of broadband teleseismic P waveforms [J]. *J Geophys Res*, **89**: 7 783~7 795.

Petersen N, Vinnik L, Kosarev G, *et al*. 1993. Sharpness of the mantle discontinuities [J]. *Geophys Res Lett*, **20**: 859~862.

WU Qing-ju, ZENG Rong-sheng. 1998. The crustal structure of Qinghai-Xizang plateau inferred from broadband teleseismic waveform [J]. *Acta Geophysics Sinica*, **41**(5): 669~679 (in Chinese).

YUAN Ya-xiang, SUN Wen-yu. 1997. *Theory and Method of Optimization* [M]. Beijing: Science Press, 219~240, 559~576 (in Chinese).

Zhao L S, Frohlich C. 1996. Teleseismic body waveforms and receiver structures beneath seismic stations [J]. *Geophys J Int*, **124**: 525~540.

# Contributors to this issue

**YU Xiang-wei** (于湘伟) Ph.D. student of Institute of Geophysics, China Seismological Bureau (IGCSB). Graduated at Speciality of Solid Geophysics, Peking University in 1997. Mainly engaged in the researches on topography of near-field earthquakes and earthquake location.

**ZOU Zui-hong** (邹最红) Graduated from Department of Geophysics, Peking University in 1999. Received her MS degree from Department of Geophysics, Peking University in 2002. Mainly engaged in the researches on seismology and interior structure of the Earth.

**ZHANG Chi-jun** (张赤军) Professor of Geodesy and Geophysics, Chinese Academy of Sciences. Received his MS degree from the Department of Geodesy, Chinese Academy of Sciences (CAS) in 1967. He has been working on the researches on gravity. Member of Geophysical Society of China and Surveying and Mapping Society of China.

**HUANG Xi-ying** (黄玺瑛) MS degree candidate majored in geophysics under the joint education of the Crustal Dynamics Institute of China Seismological Bureau and the Graduate School of CAS. Graduated from the College of Disaster Prevention Techniques in 1998. Mainly engaged in the researches on seismicity and plate tectonics.